A Crystallographic Study related to Intramolecular Hydride Shifts in Polycyclic Hydroxyketones

Robert V. Cernik, Gabrielle-Anne Craze, Owen S. Mills, Ian Watt,* and Stephen N. Whittleton
The Chemistry Department, University of Manchester, Manchester M13 9PL

The crystal structures of the *p*-nitrobenzoate (*p*-NB) esters of the hydroxyketones (1)—(3) have been determined. These contain imbedded boat-conformation 4-hydroxycyclohexanones whose C(1)–C(4) distances decrease from 2.67(3) Å in (1) (R = *p*-NB) to 2.479(6) Å in (3) (R = *p*-NB). The relationship of the structural variation to the barriers and reaction path for the 1,4-hydride transfer in the corresponding alkoxide anions is discussed.

Using data from *X*-ray crystal structures, Dunitz and his co-workers have found striking correlations between out-of-plane displacements at carbonyl groups and distances and angular relationships of these groups to closely interacting, but formally non-bonded, oxygen or nitrogen atoms in the same structures. Taken with the intuitively attractive notion that distortion of molecular fragments in response to non-bonded interactions, both inter- and intramolecular, occurs preferentially along reaction co-ordinates, these correlations have yielded useful insights into preferred pathways for attack by nucleophilic nitrogen and oxygen at the carbonyl.[1]

Our interest in intramolecular hydride transfer has led us to speculate that examination of crystal structures of molecules in which carbonyl and potential hydride source are held in close proximity by intramolecular arrangement (see Figure 1) could yield comparable information for addition to carbonyl of this simplest nucleophile.[2]

Metal-based hydride sources, *e.g.*, X = R–Al$^-$< or R–B$^-$<, are unsuitable for incorporation into the stable structures required, since they would react rapidly and exothermically with the ketonic carbonyl. Simple secondary alcohol groups, however, can readily be incorporated into molecules such as the polycyclic hydroxyketones (1)—(4) (R = H), which are well suited to structural investigation. Since this group can be activated as a hydride donor by conversion into its alkoxide, *i.e.*, X = $^-$O–C< in Figure 1, it is possible also to determine the relative facility of the hydride transfer between the alkoxide and carbonyl carbons in these structures.

Rates for such rearrangements of (1)—(3),[3] and (4) (R = Na)[4] in DMSO solution have been determined by dynamic n.m.r. methods, and despite some complications arising from association phenomena in the reactions,[5] the ordering of reactivity is clear, with (1) < (2) < (3) ≪ (4) (R = Na), with a spread of *ca.* 10^6 s^{-1}. Examination of models and empirical force-field calculation of the structures has shown clearly that there is an important non-bonded interaction between the reacting groups, and that the variation in reactivity can be related to relief of differing degrees of steric compression in the hydride transfer transition state.

Of these compounds, only the *X*-ray crystal structure of (4) [R = *p*-nitrobenzoate (*p*-NB)] has been reported.[4] Encouragingly, the central carbon of the ketonic carbonyl showed a large displacement (0.074 Å) from the plane of its ligands in the direction of the potentially hydridic methine of the secondary alcohol residue. We now describe the *X*-ray crystal structures of the *p*-nitrobenzoates of (1)—(3) and discuss some trends in the experimentally determined molecular geometry of these compounds that are possibly related to reactivity in the hydride transfer reaction.

Experimental

Preparation of (1)—(3) (R = *p*-NB).—The parent alcohols were available from earlier work.[3] Reaction with excess of *p*-nitrobenzoyl chloride in pyridine at room temperature overnight, followed by aqueous work-up, ethereal extraction, and solvent evaporation gave the crude esters. Conventional recrystallisation from anhydrous ethanol gave crystals of (2) (R = *p*-NB), m.p. 190—191 °C, and (3) (R = *p*-NB), m.p. 178—179 °C, suitable for *X*-ray crystallography. Good crystals of (1) (R = *p*-NB) proved extremely difficult to obtain. Crystallisation from hexane, cyclohexane, ether, chloroform, acetonitrile, methanol, propan-2-ol, and a range of solvent mixtures yielded small, poorly formed crystals, often growing dendritically. Controlled cooling of a solution in anhydrous ethanol eventually gave the best results giving crystals of (1) (R = *p*-NB), m.p. 150—151 °C.

Structure Determination of (1)—(3) (R = *p*-NB).—An Enraf-Nonius CAD4 four-circle diffractometer was used to measure accurate lattice parameters and for data collection. No absorption correction was applied nor was allowance made for extinction. Two standard intensity reflections were measured every 3 600 s and crystal orientations were checked every 100 reflections. The maximum counting time for any single reflection was 300 s. The structures were solved by direct methods using the MULTAN-76 suite of programs.[6] Parabolic weighting schemes of the form $\omega^{-1} = (A + B\cdot F_{obs} + C\cdot F^2_{obs})$ were applied to give uniform distributions over the F_{obs} and sin θ range with $A = 22.953$, $B = -0.4025$, $C = 0.0032$ for (1) (R = *p*-NB); $A = 0.2500$, $B = -0.0002$, $C = 0.0015$ for (2) (R = *p*-NB); $A = 1.7103$, $B = -0.1003$, $C = 0.0028$ for (3) (R = *p*-NB).

(1) (R = *p*-NB), *Crystal data.* $C_{18}H_{15}NO_5$, $M = 325$, $a = 10.140(7)$, $b = 26.158(18)$, $c = 11.608(9)$ Å, $V = 3079.7$ Å^3, *Pccn*(No. 56), $Z = 8$, $\rho_c = 1.40$, $F(000) = 1\,360$, $\lambda = 0.701\,69$ Å, $\mu = 1.23$ cm^{-1}, final $R = 0.091$ for 607 reflections with $F_{obs} > 3\sigma$.

Crystals of (1) (R = *p*-NB) were translucent colourless plates, typically with eight well formed edges. In general, the crystals were of poor quality, most consisting of several plates growing together along with [010] faces. Systematic absences from precession photography indicated the space group *Pccn*. Two crystals of dimension 0.11 × 0.22 × 0.25 mm and 0.04 × 0.09 × 0.09 mm were used in data collection. Data were collected for both crystals to a θ value of 20° using an ω/2θ scan coupled in a 1 : 2 ratio. Scan and aperture widths were (0.8 + 0.35 tanθ)° and 4 × 4 mm^2, respectively. Data from both crystals were scaled and merged; processing then yielded 607 unique reflections with $F_{obs} > 3\sigma$. Previous

knowledge of a structure thought to be stereochemically similar was used to calculate a spherically averaged scattering factor used in the normalisation process. The most likely *E*-map so obtained with 180 terms showed all non-hydrogen atoms. These co-ordinates were refined with isotropic temperature factors until convergence was reached, when the hydrogen positions were calculated and constrained to have $B = 7.5$ Å^2. The hydrogen atoms were located 1.0 Å from the adjacent carbon atoms. In the specific case of H(1), the H–C bond made equal angles with the three other bonds. Six non-hydrogen atoms with high *B* values were refined with anisotropic factors, and convergence of this model led to an *R* value of 0.091. A difference Fourier synthesis at this stage showed no peak greater than 0.4e.

Figure 3 shows a stereoscopic view of the structure, and atomic positions are given in Table 1.

(2) (R = *p*-NB), *Crystal data.* $C_{19}H_{17}NO_5$, $M = 339$, monoclinic, $a = 15.313(3)$, $b = 9.600(1)$, $c = 11.439(1)$ Å, $\beta = 110.04(2)°$, $V = 1579.7$ Å^3, $P2_1/c$ (No. 14), $Z = 4$, $\rho_c = 1.43$, $\rho_{obs} = 1.40$, $\mu = 1.25$ cm^{-1}, $\lambda = 0.710\,69$ Å, $F(000) = 712$. Final $R = 0.029$ for 1 322 reflections with $F_{obs} > 3\sigma$.

Systematic absences from precession photography led uniquely to the space group $P2_1/c$. A crystal of dimensions $0.34 \times 0.30 \times 0.13$ mm was used in the data collection. Data were collected to a θ value of 25° using an ω/2θ scan coupled

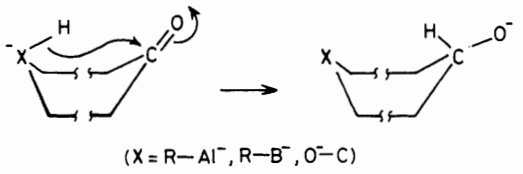

Figure 1. Intramolecular transfer of hydride to carbonyl carbon from Al, B or C

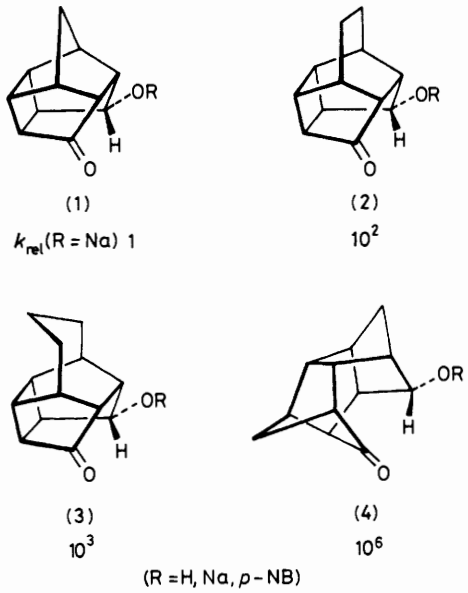

Figure 2. Structures and relative reactivities of (1)—(4)

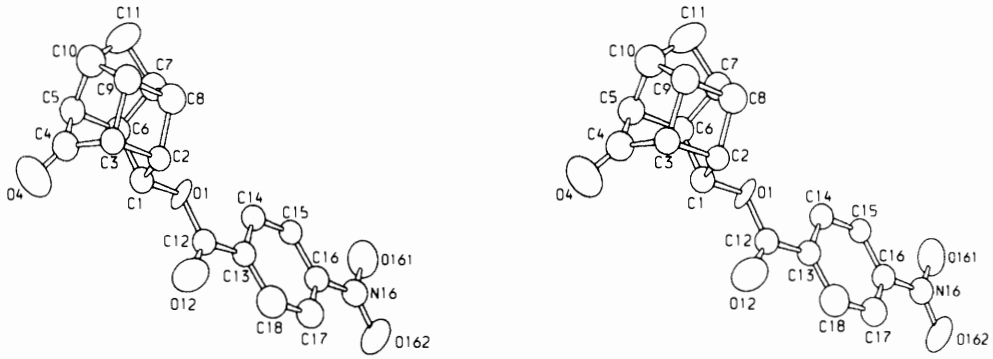

Figure 3. Stereoscopic view of the structure of (1) (R = *p*-NB)

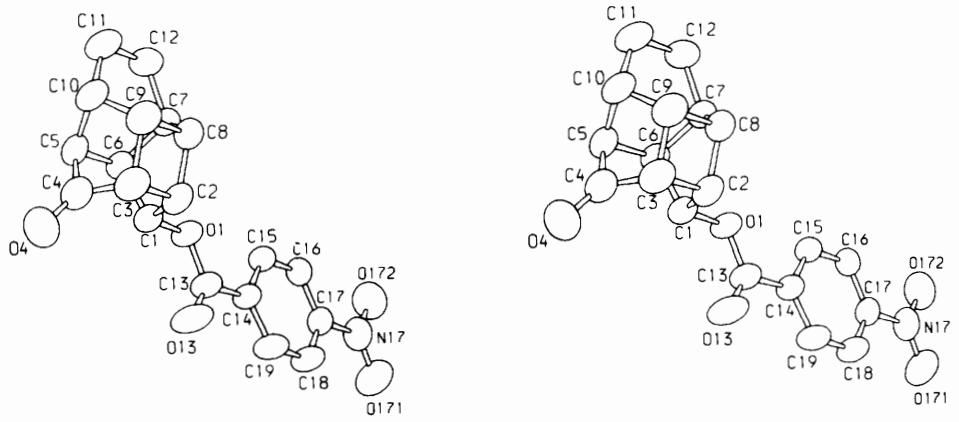

Figure 4. Stereoscopic view of the structure of (2) (R = *p*-NB)

Table 1. Atomic co-ordinates for structure of (1) (R = *p*-NB)

Atom	*x/a*	*y/b*	*z/c*
C(1)	0.009 6(17)	0.603 0(6)	0.546 5(14)
C(2)	0.063 8(16)	0.646 4(6)	0.617 4(14)
C(3)	−0.052 5(17)	0.686 9(6)	0.646 4(15)
C(4)	−0.178 7(21)	0.672 6(7)	0.581 1(16)
C(5)	−0.138 9(18)	0.673 1(6)	0.457 1(14)
C(6)	−0.022 7(18)	0.631 8(6)	0.435 0(15)
C(7)	0.098 1(18)	0.666 4(6)	0.412 7(15)
C(8)	0.133 3(18)	0.684 1(6)	0.531 7(15)
C(9)	0.023 6(19)	0.725 6(6)	0.559 6(15)
C(10)	−0.061 0(23)	0.723 7(7)	0.451 3(17)
C(11)	0.044 3(25)	0.714 3(8)	0.358 5(22)
C(12)	0.142 6(18)	0.531 0(6)	0.592 9(16)
C(13)	0.245 4(18)	0.494 8(5)	0.559 2(14)
C(14)	0.299 9(16)	0.497 1(6)	0.447 0(14)
C(15)	0.397 2(16)	0.461 0(6)	0.422 4(13)
C(16)	0.434 6(17)	0.424 0(6)	0.497 3(15)
C(17)	0.384 8(20)	0.423 7(6)	0.606 5(15)
C(18)	0.285 8(18)	0.459 6(6)	0.639 2(16)
O(1)	0.111 2(11)	0.566 5(4)	0.516 0(10)
O(4)	−0.281 7(15)	0.662 0(5)	0.629 4(14)
O(12)	0.082 4(14)	0.528 7(5)	0.686 1(10)
O(161)	0.588 7(13)	0.390 1(5)	0.369 0(14)
O(162)	0.558 6(14)	0.353 1(5)	0.538 0(13)
N(16)	0.534 5(17)	0.385 9(6)	0.467 0(13)
H(1)	−0.0728	0.5868	0.5828
H(2)	0.1195	0.6353	0.6861
H(3)	−0.0588	0.6990	0.7321
H(5)	−0.2142	0.6702	0.3991
H(6)	−0.0440	0.6079	0.3679
H(7)	0.1714	0.6493	0.3661
H(8)	0.2296	0.6936	0.5484
H(9)	0.0537	0.7607	0.5901
H(10)	−0.1182	0.7560	0.4347
H(111)	0.0058	0.7096	0.2778
H(112)	0.1126	0.7435	0.3543
H(14)	0.2684	0.5228	0.3865
H(15)	0.4443	0.4626	0.3447
H(17)	0.4209	0.3970	0.6644
H(18)	0.2456	0.4595	0.7193

Table 2. Atomic co-ordinates for structure of (2) (R = *p*-NB)

Atom	*x/a*	*y/b*	*z/c*
C(1)	−0.208 3(2)	0.012 6(3)	−0.037 8(2)
C(2)	−0.277 5(2)	0.088 3(3)	0.008 5(2)
C(3)	−0.351 3(2)	−0.018 8(3)	0.020 8(2)
C(4)	−0.329 5(2)	−0.158 1(3)	−0.022 4(3)
C(5)	−0.343 3(2)	−0.136 5(3)	−0.158 9(2)
C(6)	−0.269 5(2)	−0.026 8(3)	−0.169 8(2)
C(7)	−0.318 5(2)	0.111 3(3)	−0.218 2(2)
C(8)	−0.350 4(2)	0.151 4(3)	−0.110 0(2)
C(9)	−0.423 3(2)	0.045 0(3)	−0.098 5(3)
C(10)	−0.439 6(2)	−0.066 2(3)	−0.199 6(3)
C(11)	−0.470 7(2)	−0.006 9(4)	−0.330 1(3)
C(12)	−0.397 5(2)	0.096 2(3)	−0.342 0(2)
C(13)	−0.065 5(2)	0.126 1(3)	0.061 0(2)
C(14)	0.003 9(1)	0.229 4(3)	0.050 4(2)
C(15)	−0.003 9(2)	0.297 4(3)	−0.059 6(2)
C(16)	0.061 9(2)	0.393 8(3)	−0.062 6(2)
C(17)	0.136 0(2)	0.418 2(3)	0.044 5(2)
C(18)	0.145 3(2)	0.354 1(3)	0.154 5(2)
C(19)	0.078 5(2)	0.259 8(3)	0.156 9(2)
O(1)	−0.136 1(1)	0.106 8(2)	−0.045 1(1)
O(4)	−0.308 3(2)	−0.264 4(2)	0.037 8(2)
O(13)	−0.058 9(1)	0.066 2(2)	0.155 8(2)
O(171)	0.274 2(2)	0.535 7(3)	0.136 2(2)
O(172)	0.196 5(1)	0.581 4(2)	−0.056 0(2)
N(17)	0.207 2(2)	0.519 7(2)	0.041 1(2)
H(1)	−0.1763	−0.0684	0.0148
H(2)	−0.2510	0.1533	0.0804
H(3)	−0.3666	−0.0150	0.0990
H(5)	−0.3424	−0.2249	−0.2048
H(6)	−0.2330	−0.0625	−0.2212
H(7)	−0.2724	0.1810	−0.2262
H(8)	−0.3659	0.2518	−0.1044
H(9)	−0.4803	0.0857	−0.0880
H(10)	−0.4867	−0.1348	−0.1924
H(111)	−0.5313	0.0425	−0.3477
H(112)	−0.4784	−0.0844	−0.3913
H(121)	−0.3720	0.0614	−0.4062
H(122)	−0.4273	0.1891	−0.3683
H(15)	−0.0575	0.2764	−0.1371
H(16)	0.0558	0.4452	−0.1410
H(18)	0.1993	0.3752	0.2314
H(19)	0.0837	0.2124	0.2369

in a ratio of 1 : 2. The aperture was fixed at 4 × 4 mm ² and the scan range was given by (1.2 + 0.35 tanθ)° giving a maximum scan angle of 1.36°. The most likely *E*-map with 300 terms showed all non-hydrogen atoms whose co-ordinates were refined to convergence with isotropic temperature factors. The hydrogen atom positions were calculated and appended to the co-ordinate set. All non-hydrogen atoms were then refined with anisotropic temperature factors and hydrogen atom parameters were constrained. Subsequently an additional cycle was run with the positional parameters of 1-H freed so as to obtain an estimate of positional accuracy.

Figure 4 shows a stereoscopic view of the structure and the accompanying Table 2 gives the atomic co-ordinates.

(3) (R = *p*-NB), *Crystal data.* $C_{20}H_{19}NO_5$, monoclinic, $M = 353$, $a = 15.433(4)$, $b = 9.767(3)$, $c = 11.461(5)$ Å, $\beta = 107.41(3)°$, $V = 1\,648.4$ Å^3, $P2_1/c$ (No. 14), $Z = 4$, $\rho_c = 1.42$, $\lambda = 0.710\,69$ Å, $\mu = 1.288$ cm^{-1}, $F(000) = 744$. Final $R = 0.054$ with 1 444 reflections with $F_{obs} > 3\sigma$.

Systematic absences determined by precession photography led uniquely to the space group $P2_1/c$ and approximate lattice parameters were determined from the photographs. A crystal of dimension 0.31 × 0.26 × 0.096 mm was used in the data collection. Data were collected using an ω/2θ scan coupled in a 1 : 2 ratio to a θ value of 25°. The scan range was given by (1.0 + 0.35 tanθ)° giving a maximum scan angle of 1.16°; the detector aperture was constant at 4 × 4 mm². The *E*-map with the highest figure of merit showed all non-hydrogen atoms. From these, the hydrogen-atom positions were calculated. Hydrogen parameters were constrained and the carbon atoms given isotropic temperature factors before refining this model to convergence. Hydrogen positions were then recalculated, and a full anisotropic refinement of carbon, nitrogen, and oxygen atoms was completed. The largest thermal ellipsoid in the structure occurs in C(12), with a mean isotropic *B* value of 7.968 Å². A difference map showed an extra peak 1 Å away from C(12), and this was interpreted as the result of disorder arising from different conformations of the methylene bridge. The occupancies of the two sites C(12) and C(12′) were refined and converged with population parameters of 0.74 and 0.26, respectively. Better agreement, however, was obtained by leaving C(12) as a single atom with a large amplitude of vibration.

Figure 5 shows a stereospecific view of the structure and Table 3 lists atomic positions.

The closest heavy-atom intermolecular contacts in each of the crystal structures are listed in Table 4.

Discussion

As noted earlier, our interest centres on the relationship between molecular geometry and reactivity in intramolecular

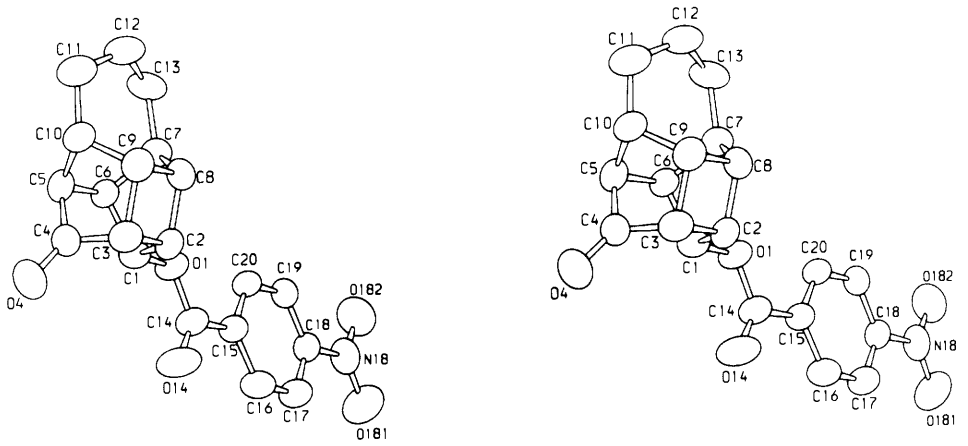

Figure 5. Stereoscopic view of the structure of (3) (R = *p*-NB)

Table 3. Atomic co-ordinates for the structure of (3) (R = *p*-NB)

Atom	*x/a*	*y/b*	*z/c*
C(1)	0.800 7(3)	0.012 4(5)	0.474 7(4)
C(2)	0.736 1(3)	0.058 9(4)	0.529 6(4)
C(3)	0.667 4(3)	−0.019 8(5)	0.552 8(4)
C(4)	0.688 7(3)	−0.154 3(5)	0.506 6(4)
C(5)	0.669 4(3)	−0.135 8(5)	0.370 8(4)
C(6)	0.737 9(3)	−0.026 5(5)	0.347 1(4)
C(7)	0.693 3(3)	0.113 3(5)	0.308 3(4)
C(8)	0.661 5(3)	0.145 5(5)	0.419 0(4)
C(9)	0.593 3(3)	0.040 8(5)	0.440 6(4)
C(10)	0.573 0(3)	−0.077 0(5)	0.349 3(4)
C(11)	0.515 8(3)	−0.048 9(6)	0.219 6(5)
C(12)	0.530 0(4)	0.078 5(7)	0.170 4(6)
C(13)	0.623 8(3)	0.125 7(6)	0.181 1(4)
C(14)	0.939 5(3)	0.124 1(5)	0.562 1(4)
C(15)	1.005 4(3)	0.229 4(4)	0.546 0(4)
C(16)	1.078 1(3)	0.259 5(5)	0.647 3(4)
C(17)	1.141 2(3)	0.355 9(5)	0.640 0(4)
C(18)	1.130 3(3)	0.418 9(4)	0.531 3(4)
C(19)	1.058 5(3)	0.393 8(4)	0.429 3(4)
C(20)	0.996 1(3)	0.295 4(4)	0.437 7(4)
O(1)	0.870 9(2)	0.104 1(3)	0.460 8(2)
O(4)	0.713 0(2)	−0.257 0(4)	0.566 7(3)
O(14)	0.946 8(2)	0.065 9(4)	0.655 7(3)
O(181)	1.262 1(3)	0.541 0(4)	0.611 5(4)
O(182)	1.184 7(3)	0.583 6(4)	0.426 6(4)
N(18)	1.197 0(3)	0.522 6(4)	0.521 9(4)
H(17)	1.1965	0.3796	0.7165
H(16)	1.0850	0.2086	0.7303
H(19)	1.0510	0.4475	0.3476
H(20)	0.9415	0.2713	0.3606
H(1)	0.8277	−0.0755	0.5253
H(2)	0.7649	0.1542	0.6015
H(3)	0.6548	−0.0162	0.6378
H(5)	0.6698	−0.2278	0.3236
H(6)	0.7735	−0.0633	0.2884
H(7)	0.7460	0.1821	0.3102
H(8)	0.6452	0.2485	0.4281
H(9)	0.5368	0.0829	0.4605
H(10)	0.5375	−0.1503	0.3841
H(131)	0.6153	0.2286	0.1526
H(132)	0.6404	0.0750	0.1102
H(121)	0.4997	0.1536	0.2111
H(122)	0.4938	0.0767	0.0768
H(111)	0.4471	−0.0550	0.2166
H(112)	0.5284	−0.1266	0.1635

Table 4. Heavy-atom intermolecular contacts <3.3 Å in the crystal structures of (1)—(3) (R = *p*-NB)

Structure	Symmetry operation between molecules A and B	Atom: Molecule A	Atom: Molecule B	*d*/Å
(1) (R = *p*-NB)	$\frac{1}{2} - x, y, z - \frac{1}{2}$	C(15) · · ·	O(12)	3.27
	$\bar{x}, 1 - y, 1 - z$	C(15) · · ·	O(4)	3.11
	$\bar{x}, 1 - y, 1 - z$	O(4) · · ·	N(16)	3.06
(2) R = *p*-NB)	$\bar{x}, 1 - y, \bar{z}$	C(8) · · ·	O(171)	3.27
	$x, \frac{1}{2} - y, z - \frac{1}{2}$	C(16) · · ·	O(13)	3.14
	$\bar{x}, \bar{y}, \bar{z}$	O(4) · · ·	N(17)	3.19
(3) (R = *p*-NB)	$x, \frac{1}{2} - y, z - \frac{1}{2}$	C(19) · · ·	O(14)	3.11
	$2 - x, \bar{y}, 1 - z$	O(4) · · ·	N(18)	3.24

1,4-hydride transfer across the hydroxycyclohexanone [C(1), C(2), C(3), C(4), C(5), C(6), O(1), and O(4)] imbedded in each of these structures. In these polycyclic molecules, the conformation of this ring will be determined by a balance of intra- rather than inter-molecular forces. Interestingly, although (1) (R = *p*-NB) crystallises in a different space group, all three structures have, amongst their closest intermolecular contacts (Table 4), those between a ketonic oxygen and the nitrogen of another *p*-nitrobenzoate. The distances, however, are all longer than the sum of the van der Waals radii for these atoms (2.9 Å) [7] and should not be taken as indicative of a strong interaction.

As expected from molecular modelling and empirical force field calculation,[8] the hydroxycyclohexanone rings are held in recognisable boat conformations with the oxygen-bearing sites [C(1) and C(4)] at the prow and stern positions. Figure 6 shows detail of these rings, and Table 5 collects relevant structural data. In all the structures, the boats have a slight twist, shown by the C(1)–C(2)–C(3)–C(4) and C(4)–C(5)–C(6)–C(1) torsion angles, with the result that the atoms involved in the potential hydride transfer [O(1), C(1), H(1), C(4), and O(4)] are not truly coplanar. Deviations from the mean plane are all less than 0.05 Å, with the largest occurring in (1) (R = *p*-NB).

The hydrocarbon cages, which differ only in the lengths of a remote methylene bridge [C(11) in (1), C(11)–C(12) in (2) and C(11)–C(12)–C(13) in (3) (R = *p*-NB)], may be regarded as electronically constant sets of substituents acting to modify the conformation of hydroxycyclohexanones. The small differences are not immediately obvious from the diagrams, but are revealed by the tabulated data. Expansion of the

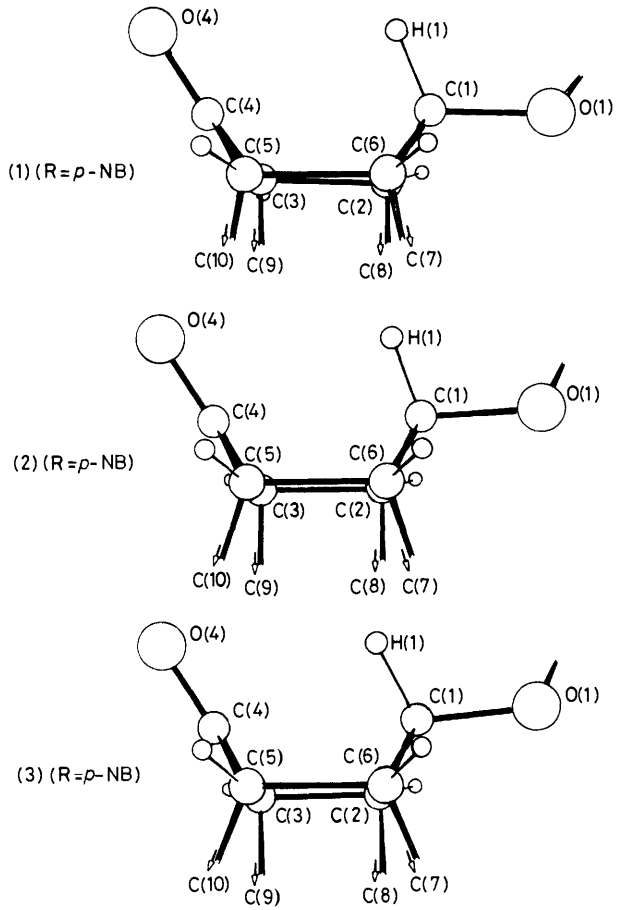

Figure 6. Details of the hydroxycyclohexanone ring in the structures of (1), (2), and (3) (R = *p*-NB)

bridges primarily affects the separation of the bridgehead atoms, C(7) and C(10), which increases from 2.25 Å in (1) to 2.762 Å in (3), and can be seen in Figure 6 by the increasing splay of the exocyclic bonds from C(6) and C(5) to these atoms. Transmission of these changes [9] to the six-membered rings occurs most obviously through close non-bonded approaches between the C(7) bridgeheads and the alcoholic oxygens, O(1), which decrease from 2.88 Å in (1) to 2.77 Å in (3) (R = *p*-NB), and the decreasing pyramidalization at C(1) in the series, measured by displacement of C(1) from the plane of O(1), C(2), and C(6), seems to be a response to the increasing non-bonded repulsions between C(7) and O(1). The C(1)–O(1) bond lengths do not vary significantly in these esters, and are all slightly longer than the average [1.445(12) Å] found in a range of secondary aromatic esters.[10]

Within the six-membered ring, the lengths of the C(2)–C(3) bonds, common to the cyclobutane rings, decrease with extension of the methylene bridge. At its longest, in (1), this bond length is significantly longer than the 1.55—1.56 Å commonly found in cyclobutane derivatives.[11] A similar but less emphatic trend is found in the lengths of the C(3)–C(4) and C(5)–C(6) bonds. In general, the differences between the rings in (1) and (2) are more pronounced than those between (2) and (3), a feature of the series well reproduced by molecular mechanics calculations.[12]

The cumulative effect of the structural changes in the series (1)—(3) is motion of the potential hydride-donating group, O(1)–C(1)–H(1), towards its accepting carbonyl partner, C(4)=O(4), with relatively little change of angular

Table 5. Selected parameters from structures of (1), (2), and (3) (R = *p*-NB)

Parameter	(1) (R = *p*-NB)	(2) (R = *p*-NB)	(3) (R = *p*-NB)
(*a*) Bond lengths (Å)			
C(1)–C(2)	1.51(2)	1.522(3)	1.510(6)
C(2)–C(3)	1.62(2)	1.570(3)	1.560(6)
C(3)–C(4)	1.53(2)	1.503(4)	1.490(7)
C(4)–C(5)	1.50(2)	1.516(4)	1.505(6)
C(5)–C(6)	1.62(2)	1.580(3)	1.582(6)
C(6)–C(1)	1.55(2)	1.531(3)	1.534(6)
C(1)–O(1)	1.45(2)	1.453(3)	1.452(5)
C(4)–O(4)	1.22(2)	1.212(3)	1.212(6)
C(1)–H(1)	1.03 [a]	1.002 [a]	1.050 [a]
(*b*) Bond angles (°)			
C(6)–C(1)–C(2)	100(1)	101.4(2)	101.9(3)
C(1)–C(2)–C(3)	110(1)	109.1(2)	108.9(4)
C(2)–C(3)–C(4)	110(1)	107.7(2)	106.8(4)
C(3)–C(4)–C(5)	104(2)	104.5(2)	105.4(4)
C(4)–C(5)–C(6)	110(2)	108.8(2)	108.9(3)
C(5)–C(6)–C(1)	110(1)	107.4(2)	105.4(3)
O(1)–C(1)–C(2)	112(2)	110.9(2)	111.1(4)
O(1)–C(1)–C(6)	106(1)	108.5(2)	109.0(3)
O(1)–C(1)–H(1)	114 [a]	107.0 [a]	112.3 [a]
O(4)–C(4)–C(3)	123(2)	127.5(3)	126.3(4)
O(4)–C(4)–C(5)	133(2)	128.1(3)	128.3(5)
(*c*) Torsion angles (°)			
C(6)–C(1)–C(2)–C(3)	67	68	69
C(1)–C(2)–C(3)–C(4)	−7	−2	−3
C(2)–C(3)–C(4)–C(5)	−58	−64	−65
C(3)–C(4)–C(5)–C(6)	60	64	65
C(4)–C(5)–C(6)–C(1)	2	2	3
C(2)–C(1)–C(6)–C(5)	−65	−67	−67
O(1)–C(1)–C(2)–C(3)	−178	−177	−175
O(1)–C(1)–C(6)–C(5)	179	177	175
O(1)–C(1)–C(2)–C(8)	79	89	89
O(1)–C(1)–C(6)–C(7)	−72	−68	−68
O(4)–C(4)–C(5)–C(6)	−117	−118	−118
C(2)–C(3)–C(4)–O(4)	119	118	118
O(4)–C(4)–C(3)–C(9)	−150	−149	−149
O(4)–C(4)–C(5)–C(10)	137	129	126
(*d*) Intramolecular non-bonded distances (Å)			
C(1) · · · C(4)	2.67(3)	2.526(4)	2.479(6)
C(1) · · · O(4)	3.47(2)	3.327(3)	2.274(6)
C(4) · · · H(1)	2.49 [a]	2.40(2)	2.30(4)
C(4) · · · O(1)	4.11(2)	3.979(3)	3.929(6)
H(1) · · · O(4)	2.94 [a]	2.840 [a]	2.647 [a]
O(1) · · · C(7)	2.88(2)	2.817(3)	2.777(5)
O(1) · · · C(8)	3.09(2)	3.137(3)	3.148(5)
O(1) · · · O(4)	4.88(2)	4.720(3)	4.650(6)
O(4) · · · C(9)	3.61(2)	3.531(4)	3.516(6)
O(4) · · · C(10)	3.45(3)	3.360(4)	3.278(6)
C(7) · · · C(10)	2.25(3)	2.580(4)	2.762(6)
(*e*) Other parameters			
C(1) [O(1), C(2), C(6)] (Å) [b]	0.579	0.557	0.548
C(4) [O(4), C(3), C(5)] (Å) [b]	−0.021(20)	0.014(4)	0.019(5)
C(1)–H(1) · · · C(4) (°)	89	86	91
H(1) · · · C(4)–O(4) (°)	99	98	96

[a] Indicates constrained parameter. [b] Positive values indicate displacements towards H(1).

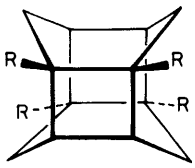

(R = Me, CO_2H)

(5)

relationships within these groups. Angles at the hydrogen, C(1)–H(1)···C(4), range from 86 to 91°, and 'angles of attack' by hydride at carbonyl are between 99 and 96°. (These angles are, of course, largely determined by the constraints of the cage structures, and not indicative of a preference in the hydride transfer reaction.) Corresponding to an increase in reactivity of *ca.* 10^3 in the alkoxides (1)—(3) (R = Na), C(1)···C(4) non-bonded distances in the *p*-nitrobenzoates decrease from 2.67 Å in (1) to 2.479 Å in (3). These are relatively close contacts, and may be compared with the corresponding distances of from 2.77 to 2.82 Å in the boat cyclohexanes in the tetra-asterane derivatives, (5),[13] while 1,4-distances in less highly constrained cyclohexanes are more typically close to 2.9 Å. H(1)···C(4) distances run from 2.49 Å in (1) to 2.297 Å in (3) (R = *p*-NB), all larger than the corresponding distance (2.18 Å) in (4) (R = *p*-NB), whose alkoxide is *ca.* 10^3 times more reactive than (3) (R = Na), although its C···C distance is actually larger (2.583 Å) because of the different angular arrangement of the reacting groups in this structure. In the *p*-nitrobenzoates, H(1) will have little hydride character and, at these distances, the H···C=O non-bonded interaction should be repulsive. Intramolecular non-bonded repulsions are notoriously difficult to quantify,[14] but expressions from current force fields, including those of White and Bovill,[15] Allinger *et al.*,[16] or Ermer and Lifson [17] all show that the repulsions in (1) and (4) (R = *p*-NB) differ by less than 2.5 kcal mol^{-1}. Although the trend is correct, this difference is not large enough to account fully for the wide spread in reactivity in the alkoxides in terms of loss of this repulsion in the hydride transfer transition state. Additional factors, such as relaxation of other ground-state strains and possible strain in the transition state have to be invoked. Calculation on a range of transition state models will be reported separately.

The ketonic carbonyls in both (2) and (3) (R = *p*-NB) show small significant pyramidalizations (0.014 and 0.019 Å, respectively) with the central carbon apparently displaced from the plane of its ligands towards the potentially hydridic hydrogen, H(1). The carbonyls are not involved in any close non-bonded contacts other than those with C(1) and H(1), and distortions from their expected planar arrangements can reasonably be associated with this interaction, although, in view of the likely repulsive nature of the interaction, they might better be described as displacements of the ketonic oxygen away from the C–H group. The pyramidalizations in (2) and (3) (R = *p*-NB) do not differ significantly, and we point out that (3) (R = Na) is only *ca.* 10 times more reactive than (2) (R = Na). Unfortunately, through no lack of preparative or crystallographic effort, the structure of (1) (R = *p*-NB), with the least reactive alkoxide, is not sufficiently determined to justify inclusion of its pyramidalization in any comparison. However, the carbonyl pyramidalizations in (1)—(3) (R = *p*-NB) are all less than that (0.074 Å) found in (4) (R = *p*-NB), which has, by far, the most reactive alkoxide.

The structural data on the *p*-nitrobenzoates suggest, qualitatively, a correlation between the H···C=O non-bonded distances and carbonyl pyramidalization and comparison may be made with the well studied behaviour [1] of amino ketones in which an amine lone pair is directed towards carbonyl carbon. In these structures, the N···C=O interaction is regarded as attractive, and the nitrogen to carbon distance (*d*) and carbonyl pyramidalization (Δ) are correlated by expression (i)

$$d = -1.701 \log \Delta + 0.867 \text{ Å} \quad \text{(i)}$$

Our data suggest that when a tertiary amine nitrogen and its lone pair are formally replaced by a C–H group, with a repulsive interaction with the carbonyl, the structural response of the carbonyl is also in the sense expected for an adjustment of molecular geometry along the reaction coordinate for nucleophilic attack at the carbonyl. Equally important, the combined structural and kinetic studies on these molecules now support a link between the experimentally determined structural features in the 'static' crystal structures and the 'dynamics' of the closely related reacting systems.

The thermal parameters and structure factors are contained in Supplementary Publication No. SUP 23828 (38 pp.).*

Acknowledgements

We thank the S.E.R.C. for support and Professor J. D. Dunitz, E.T.H. Zürich, for valuable comments.

References

1 For full discussion and references to primary literature see J. D. Dunitz, 'X-Ray Analysis and the Structure of Organic Molecules,' Cornell U.P., Ithaca, New York, 1979, pp. 366—368.
2 (*a*) P. Murray-Rust, J. Murray-Rust, W. Parker, R. L. Tranter, and I. Watt, *J. Chem. Soc., Perkin Trans. 2*, 1979, 1496; (*b*) G.-A. Craze and I. Watt, *J. Chem. Soc., Chem. Commun.*, 1980, 147.
3 G.-A. Craze and I. Watt, *J. Chem. Soc., Perkin Trans. 2*, 1981, 175.
4 R. Cernik, G.-A. Craze, O. S. Mills, and I. Watt, *J. Chem. Soc., Perkin Trans. 2*, 1982, 361.
5 G.-A. Craze and I. Watt, *Tetrahedron Lett.*, 1982, **23**, 975.
6 G. Germain, P. Main, and M. M. Woolfson, *Acta Crystallogr.*, 1971, **A27**, 368.
7 L. Pauling, 'The Nature of the Chemical Bond,' Cornell U.P., Ithaca, New York, 1960, 3rd edn., pp. 257—264.
8 Details are given in refs. 3 and 4.
9 D. H. R. Barton, A. J. Head, and P. J. May, *J. Chem. Soc.*, 1957, 935.
10 W. B. Schweizer and J. D. Dunitz, *Helv. Chim. Acta*, 1982, **65**, 1547.
11 J. D. Dunitz and V. Schomaker, *J. Chem. Phys.*, 1952, **20**, 1703.
12 (*a*) See ref. 4; (*b*) J. C. Barborak, D. Khoury, W. F. Maier, P. v. R. Schleyer, E. C. Smith, jun., and C. Wyrick, *J. Org. Chem.*, 1979, **44**, 4761.
13 (*a*) J. P. Cheswick, J. D. Dunitz, U. v. Gyzycki, and H. Musso, *Chem. Ber.*, 1973, **106**, 15; (*b*) H. G. Fritz, H. M. Hulmacher, H. Musso, G. Ahlgren, B. Akermark, and R. Karlsson, *Chem. Ber.*, 1976, **109**, 3781.
14 See comment by N. L. Allinger, *Adv. Phys. Org. Chem.*, 1976, **13**, 15.
15 D. N. J. White and M. J. Bovill, *J. Chem. Soc., Perkin Trans. 2*, 1977, 1610.
16 N. L. Allinger, M. T. Tribble, and M. A. Miller, *Tetrahedron*, 1972, **28**, 1173.
17 O. Ermer and S. Lifson, *J. Am. Chem. Soc.*, 1973, **95**, 4121.

Received 28*th July* 1983; *Paper* 3/1314

* For details of the Supplementary Publication Scheme see Instructions for Authors, *J. Chem. Soc., Perkin Trans. 2*, 1984, Issue 1.